Science of the Total Environment 651 (2019) 3127–3138

Contents lists available at ScienceDirect

Science of the Total Environment

journal homepage: www.elsevier.com/locate/scitotenv

Multiple methods for the identification of heavy metal sources in cropland soils from a resource-based region

Bo Dong [a,b,1], Renzhi Zhang [a,*], Yandong Gan [c,d,**,1], Liqun Cai [a], Ariel Freidenreich [e], Kepeng Wang [a], Tianwen Guo [b], Hongbin Wang [f]

[a] College of Resources and Environmental Sciences, Gansu Agricultural University, Lanzhou 730070, China
[b] Dryland Agriculture Institute, Gansu Academy of Agricultural Sciences, Lanzhou 730070, China
[c] Environment Research Institute, Shandong University, Qingdao 266237, China
[d] Tropical Research & Education Center, University of Florida, Homestead 33031, USA
[e] Department of Earth and Environment, Florida International University, Miami 33199, USA
[f] Shandong Agricultural Broadcasting and Television School, Jinan Branch, Jinan 250002, China

HIGHLIGHTS

- Six methods were compared for source identification of heavy metals in soils.
- 95% of As came from wastewater irrigation.
- 75, 88, 60, and 76% of Cr, Mn, Ni, and V were derived from natural origins.
- 81, 93, and 70% of Cu, Pb, and Zn originated from industrial sources.
- Natural origins, industrial sources, and wastewater irrigation were main sources.

GRAPHICAL ABSTRACT

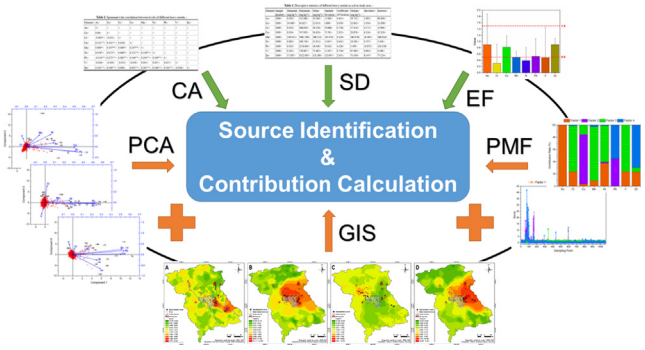

ARTICLE INFO

Article history:
Received 14 June 2018
Received in revised form 18 September 2018
Accepted 10 October 2018
Available online 11 October 2018

Editor: Xinbin Feng

Keywords:
Loess Plateau
Heavy metal
Positive matrix factorization (PMF)
Soil pollution
Source appointment

ABSTRACT

Examination of heavy metal sources in soils from a resource-based region is essential for source identification and implementation of restoration strategies regarding soil contamination. A total of 1069 samples were collected from cropland soils in the Baiyin District (Loess Plateau, Northwest China), a characteristically resource-based region to investigate the sources of arsenic (As), chromium (Cr), copper (Cu), manganese (Mn), nickel (Ni), lead (Pb), vanadium (V), and zinc (Zn). Source identification was analyzed by multiple methods including spatial deviation (SD), correlation analysis (CA), enrichment factor (EF), principal component analysis (PCA), geographic information system (GIS), and positive matrix factorization (PMF). The results showed the combined applications of PMF, GIS, and PCA were accurate, pragmatic, and effective for source apportionment. Three origins were identified and the contribution rates were calculated as follows: approximately 95% of As came from wastewater irrigation; 75, 88, 60, and 76% of Cr, Mn, Ni, and V were separately derived from natural origins; and 81, 93, and 70% of Cu, Pb, and Zn originated from industrial sources, respectively. Natural origins, industrial sources, and wastewater irrigation were the three main contributors of heavy metals to cropland soils in this region.

* Correspondence to: R. Zhang, College of Resources and Environmental Sciences, Gansu Agricultural University, No. 1 Yingmen village, Lanzhou 730070, China.
** Correspondence to: Y. Gan, Environment Research Institute, Shandong University, Binhai Road 72, Qingdao, Shandong 266237, China.
E-mail addresses: zhangrz@gsau.edu.cn (R. Zhang), sdugyd@aliyun.com (Y. Gan).
[1] These authors contributed equally to this work and should be considered co-first authors.

https://doi.org/10.1016/j.scitotenv.2018.10.130
0048-9697/

1. Introduction

Heavy metal accumulations in the soil are greater in resource-based areas because of long-term pollution emissions (Chakraborty et al., 2017; Yang et al., 2018). Although pollution activities have ceased, the residual contamination of heavy metals will persist for long periods (Han et al., 2018), which poses a constant threat to the environment and human health (Gabarrón et al., 2018; Lü et al., 2018). These elements originate not only from human activities, but also from natural factors including weathering, precipitation, and atmospheric sedimentation (Luque-Espinar et al., 2018). It is crucial to distinguish various sources of heavy metals in croplands (Franco-Uría et al., 2009), which is beneficial for devising and implementing restoration strategies in contaminated regions.

Multiple methods, such as spatial deviation (SD), correlation analysis (CA), enrichment factor (EF), principal component analysis (PCA), and geographic information system (GIS) have been used to find the distinct sources of heavy metals in soils (Das et al., 2018; Facchinelli et al., 2001; Franco-Uría et al., 2009; Gu et al., 2012; Gu et al., 2014). These approaches can quickly identify the common features of new components by classification or dimension reduction (Ha et al., 2014; Huang et al., 2007; Song et al., 2018). Accurate tracking and precise calculation of contribution rates, however, cannot be achieved through these methods (Tian et al., 2018). Positive matrix factorization (PMF), recommended by the U.S. EPA, is an ideal receptor model for source identification and quantification (Guan et al., 2018; X. Zhang et al., 2018), that decomposes the original dataset into a contribution matrix and a profile group for contribution calculation and source appointment (U.S. EPA, 2014). Combining the PMF model with GIS, the applications would serve as an effective tool for identifying contamination (Guan et al., 2018). However, few studies revealed the comparison of the various approaches based on those polluted regions.

Baiyin (also known as "copper city") is an important base of nonferrous metals in the Loess Plateau of Northwest China, with abundant reserves of Cu, Zn, Pb, Mn, Au, and Ag (Li et al., 2006; Yang et al., 2018). The district was named "silver" (in Chinese) because of the flourishing mining and smelting that occurred 600 years ago (Baiyin District Portal, 2017). The metal-related industry has grown exponentially since the 1960s causing severe contamination of soils and agricultural products via wastewater and particle settlement (Chen et al., 2018; Hu and Nan, 2018; Q. Zhang et al., 2018), which threaten the local environment and human health (Han et al., 2018; Hu et al., 2017). A 2015 project funded by the Chinese Ministry of Environmental Protection revealed that Baiyin ranked number one for the critical areas in need of control and remediation of heavy metals (CNMF and CNMEP, 2015). The severity of heavy metal pollution in this area has aroused great concern in public.

For decades, portable X-ray fluorescence spectrometry has proven useful for quantifying elements in water, plant, and soil materials (Cai et al., 2015; McGladdery et al., 2018; Pearson et al., 2018). However, this method is not ideal due to the high limit of detection (LOD) (CNMEP, 2015). These instruments are convenient and efficient owing to their ability to determine elements such as As, Co, Cr, Cu, Mn, Ni, Pb, V, and Zn, which have high concentrations in soil.

The objectives of our study were to 1) explore the sources of arsenic (As), chromium (Cr), copper (Cu), manganese (Mn), nickel (Ni), lead (Pb), vanadium (V), and zinc (Zn) in cropland soils from a resource-based region by multiple methods; 2) compare the differences among these targeted methods determining a scientific and rational approach for source identification; and 3) to quantify the origins of the selected metals in the study area for guiding restoration strategies.

2. Materials and methods

2.1. Study area

The Baiyin District, a resource-based region with a long history of mining and smelting, is the focus area for this study because the soil has been contaminated with various heavy metals (Li et al., 2006; Yang et al., 2018). This region (36°14′38″N–36°47′29″N 103°53′24″E–104°24′55″E) is situated in the continental arid and semi-desert climate zone, exhibiting typical characteristics of sparse rainfall, high evaporation, adequate sunshine, drought and frequent winds (*Wikipedia*, 2018). The primary soils are calcite soil, silty soil, and red clay, derived from Loess parent material, Yellow River alluvial deposits and red soil parent material, respectively (Baiyin District Portal, 2017). The mining and smelting industry started 600 years ago and developed rapidly in the 1960s due to the abundant mineral reserves. Intensive mining gradually decreased with the depletion of mineral resources after 2010 (Yang et al., 2018). This is a typical development path of resource-based cities in many parts of the world (Chakraborty et al., 2017; Ha et al., 2014). Long-term pollutant emissions and wastewater irrigation in this dry climate led to severe heavy metal contaminations in farmland soils and agricultural products (Hu and Nan, 2018; Li et al., 2006; Liu, 2003; Nan et al., 2002; Nan and Zhao, 2000; Q. Zhang et al., 2018).

2.2. Sampling and analytical procedure

Based on the characteristics of representative units such as the size of cultivated land, topographic features, and soil type, 1069 samples were collected in 2013 within the cropland of this study area (Fig. 1). Accurate coordinates for each unit were recorded using a portable global positioning system instrument (GPS72H, Garmin, Taipei, China) and added to the spatial database. Topsoil (0–20 cm) was collected using a stainless steel drill; 15 subsamples were mixed for the large unit with variable terrain and 5 subsamples for the small area with gentle terrain. The "S-shaped sampling" method was conducted for the former, and the coordinates were located at the point with the most dominant representative. For the latter, five sampling points were selected, and the coordinates were located in the middle (Edwards, 2010).

The soil samples were air-dried in the laboratory at room temperature (approximately 25 °C), then ground by an agate mortar to pass through a 0.075-mm nylon sieve. Approximately 4.0 g of powder sample was squeezed under 40 tons of pressure for 20 s, creating a compressed specimen with a thickness of 4 mm and a diameter of 30 mm. The total contents of As, Co, Cr, Cu, Mn, Ni, Pb, V, and Zn were determined with high-accuracy portable X-ray fluorescence spectrometry (X-MET7000, Oxford Instruments, High Wycombe, England) (Carr et al., 2008; Tighe et al., 2018), with the limits of detection (LODs) of 1.600, 1.600, 1.100, 1.200, 10.000, 1.000, 1.000, 1.400, and 2.000 mg kg^{-1}, respectively.

In addition, the certified reference soil (GBW07454) from the China Standard Material Center was analyzed for use as a quality control standard. The average recoveries for As, Co, Cr, Cu, Mn, Ni, Pb, V, and Zn in the certificated reference soil were 95.77, 100.84, 94.38, 95.27, 103.69, 96.72, 95.62, 94.87, and 101.45%, respectively, which the detected concentrations of the certified reference soil were not beyond the given ranges.

2.3. Data analysis

As an independent sample nonparametric method, Spearman's rho correlation was performed to explore the relationships among the heavy metals (Gan et al., 2017). Enrichment factor (EF) was established to trace the elemental sources of atmospheric particulates (Zoller et al., 1974) and was extended to the domain of heavy metals in the soil (Gu et al., 2012).

$$EF = \left(C_i/C_{ref}\right)_{sample} / \left(C_i/C_{ref}\right)_{background} \quad (1)$$

where C_i and C_{ref} are the concentrations of element i and reference element (Co was selected as the reference element in this study); *sample* and *background* denote the values in the sample and background, respectively. Principal component analysis (PCA) was utilized to summarize the common patterns of the heavy metals and then to

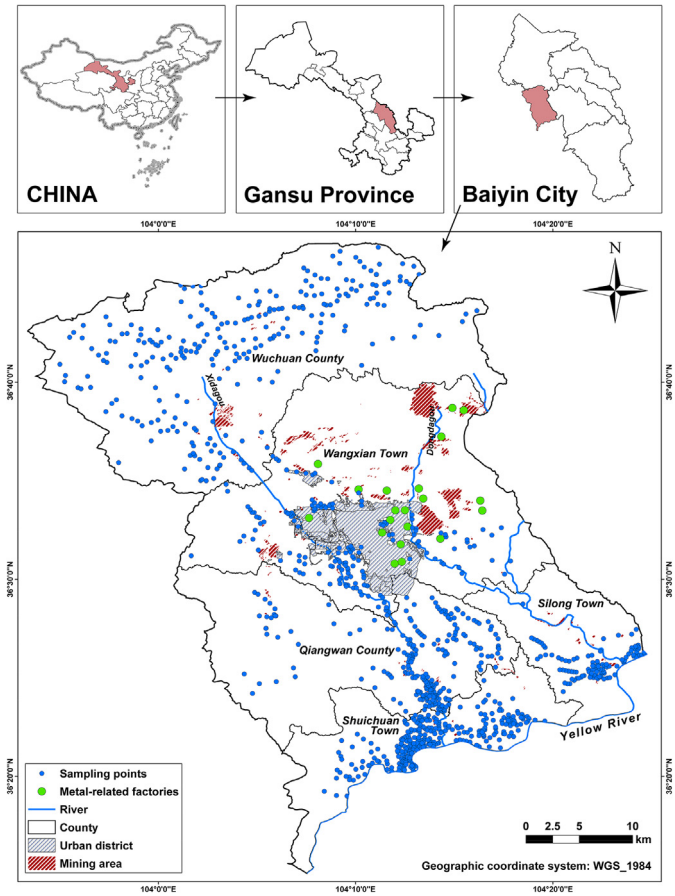

Fig. 1. Map of study area in Baiyin District, Northwest China.

identify the sources of new components (Ha et al., 2014). Data analyses were performed using SPSS Statistics 22 (IBM, Armonk, NY).

Ordinary Kriging interpolation was executed in GIS (ArcGIS 10, ESRI, Redlands, CA) to construct spatial distribution maps for principal components and levels of heavy metals (Krivoruchko, 2011). As a factor analysis tool, PMF (PMF 5.0, U.S. EPA, Washington, DC) was manipulated to identify sources and measure contributions by decomposing the sample data into source contributions and factor profiles (U.S. EPA, 2014). All plots were drawn in OriginPro 2015 (OriginLab, Northampton, MA).

3. Results and discussion

3.1. Spatial deviation

Table 1 shows that the mean concentrations of As, Co, Cr, Cu, Mn, Ni, Pb, V, and Zn in soils were 20.584, 22.914, 39.118, 36.650, 588.513, 25.012, 18.400, 71.482, and 113.580 mg kg^{-1}, respectively, with the order of Mn > Zn > V > Cr > Cu > Ni > Co > As > Pb. A previous study revealed that heavy metals in soil within this area followed the sequence of Zn (230.66 mg kg^{-1}) > Pb (100.7 mg kg^{-1}) > Cu (60.05 mg kg^{-1}), which differed from the current outcomes due to more widespread sampling sites of the current study (Dai et al., 2012).

The large standard deviation and coefficient of variation for Cu (73.761, 2.013), Pb (76.102, 4.136), and Zn (232.907, 2.051) suggested that these three elements had relatively high spatial variation (Jia et al., 2018) and had been elevated at contaminated locations by external inputs, such as human activities and atmospheric deposition (Tume et al., 2018). Additionally, the average values of Cu, Pb, and Zn were much higher than the median, whereas smaller differences existed for the other elements, making abnormal distributions of the concentrations with positive skewness and cliffy kurtosis. These results provided further evidence for the external inputs of Cu, Pb, and Zn in soils.

Among all tested elements, Co was unique for the lowest standard deviation (0.898) and the smallest coefficient of variation (0.039). This element served as a reference due to its uniform distribution in the soil with less external influence (Ranjan et al., 2018; Tume et al., 2018).

3.2. Correlation analysis

Spearman's rho correlation, a nonparametric method, was adopted to explore the relationships between selected heavy metals. As demonstrated in Fig. 2, significant positive relations are found among Cu, Pb, and Zn, confirming the common behavior of the three metals in this area, which is supported by the spatial deviation. Previously, the elevated presence of Cu, Pb, and Zn have been associated with human activities, such as mining and smelting factories, coal-fired power plants, and industrial parks (Ha et al., 2014; Hu and Cheng, 2013; Yoon et al., 2006).

Positive relationships were also found between Co and Cu, Mn, Pb, and Zn. Due to the uniform distribution of Co, these results suggested that the latter four elements occurred naturally in the soil via the parent materials and mineral constituents (Lü et al., 2018). The study area is located on the Baiyin-Qingshuigou-hangma polymetallic deposit, a crucial metallogenic belt in Northwest China established from volcanic activities during the Silurian period, causing Cu, Zn, Pb, and Mn to be naturally abundant (Tang et al., 2002).

In contrast to the synergism of other metals, As and Pb were negatively correlated with a coefficient of −0.454, indicating two different sources. Generally, As in the soil is sourced from agrochemicals, irrigation waters, and atmospheric deposition (X. Zhang et al., 2018), whereas Pb is rooted in mineral soils and enriched following mining and smelting activities (Kabata-Pendias, 2011).

The results also revealed that V had no apparent correlations with other metals. Similar to Co, V was uniformly distributed throughout the soil, sourcing from mafic igneous rocks (Kabata-Pendias, 2011).

3.3. Enrichment factor

The EF value for specific tested metals was regarded as an indicator for different sources, including natural weathering

Table 1
Descriptive statistics of different heavy metals in soil at study area (n = 1069).

Element	<LOD[a] quantity	Minimum (mg kg^{-1})	Maximum (mg kg^{-1})	Mean (mg kg^{-1})	Standard deviation	Coefficient of variation	Median (mg kg^{-1})	Skewness	Kurtosis
As	17	–	211.060	20.584	13.400	0.651	19.731	5.605	60.000
Co	0	19.489	30.627	22.914	0.898	0.039	22.842	1.916	12.098
Cr	34	–	168.630	39.118	29.668	0.758	37.424	0.572	−0.084
Cu	11	–	747.091	36.650	73.761	2.013	20.876	6.116	42.330
Mn	0	236.415	5982.590	588.513	193.470	0.329	580.078	20.495	566.916
Ni	7	–	106.716	25.012	11.047	0.442	24.585	0.737	3.419
Pb	48	–	1156.604	18.400	76.102	4.136	3.499	10.871	136.538
V	53	–	278.607	71.482	51.197	0.716	67.485	0.602	0.180
Zn	0	17.387	3322.065	113.580	232.907	2.051	71.436	8.147	77.124

[a] LOD = limit of detection. The number of samples that below LOD are <5%.

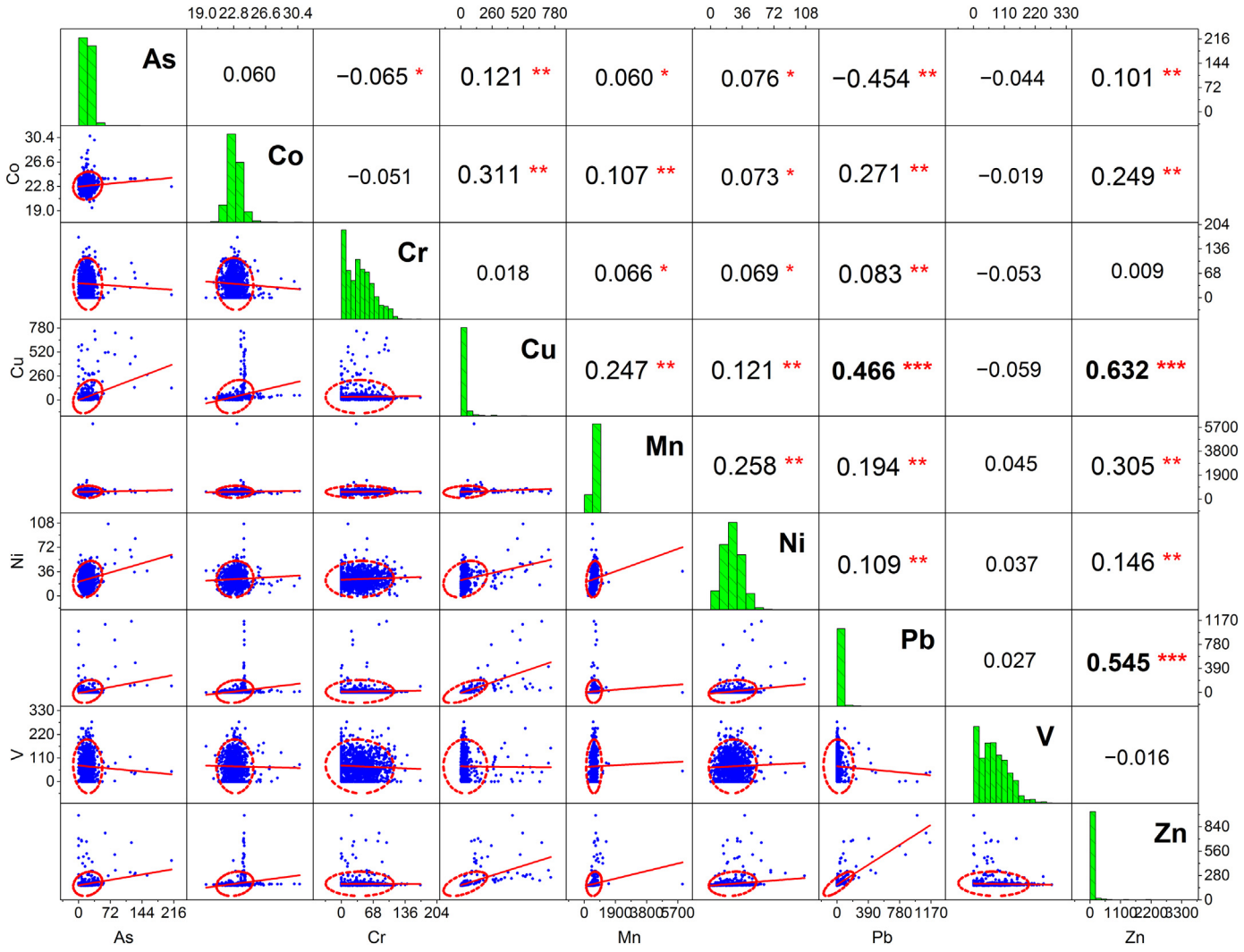

Fig. 2. Relationships between different elements in soils using scatter matrix analysis.

processes or anthropogenic sources (Gu et al., 2012). The value of EF < 0.5 indicates the source originated from the Earth's crust, whereas 0.5 ≤ EF ≤ 1.5 denotes a natural contribution and related human activities (mining and smelting), and EF > 1.5 signifies point and non-point pollution (Zhang and Liu, 2002). Cobalt was selected as the reference element because of its low deviation and uniform distribution. The average values of EF for each element were calculated based on the background values (As 12.6, Cr 70.2, Cu 24.1, Mn 653, Ni 35.2, Pb 18.8, V 81.9, Zn 68.5, Co 12.6 mg kg^{-1}) (CNEMC, 1990).

As illustrated in Fig. 3, the average values of EF for Zn (0.912), As (0.898), Cu (0.836), and Pb (0.538) are larger than 0.5, showing the natural and anthropogenic origins of the four metals, whereas the remaining elements, Mn (0.496), V (0.480), Ni (0.391), and Cr (0.306) are originated from the Earth's crust. However, these results differed from the correlation analysis, because the reference element, Co (22.914 mg kg^{-1}), was 1.819 times greater than the background value (12.6 mg kg^{-1}), causing smaller EF values than expected. Accordingly, the adjusted classification made them appropriate that Zn, As, Cu, and Pb were from anthropogenic sources, Mn, V, and Ni were from natural weathering processes, and Cr was from the Earth's crust. The artificial origins included both agricultural sources (fertilization and irrigation) for As and industrial sources (mining and smelting) for Pb, despite the results of correlation analysis (Du et al., 2017).

3.4. Principal component analysis

As an approach of dimension reduction, PCA utilizing non-rotation method was selected to find common characteristics in concentration

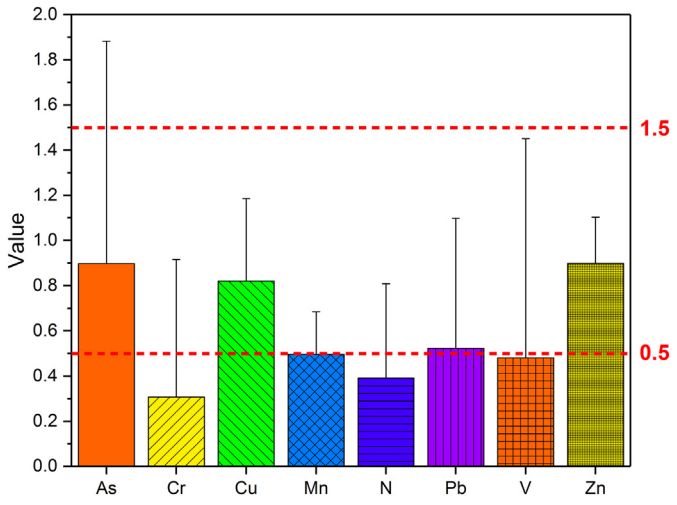

Fig. 3. Values of enrichment factor (EF) for heavy metals in soil.

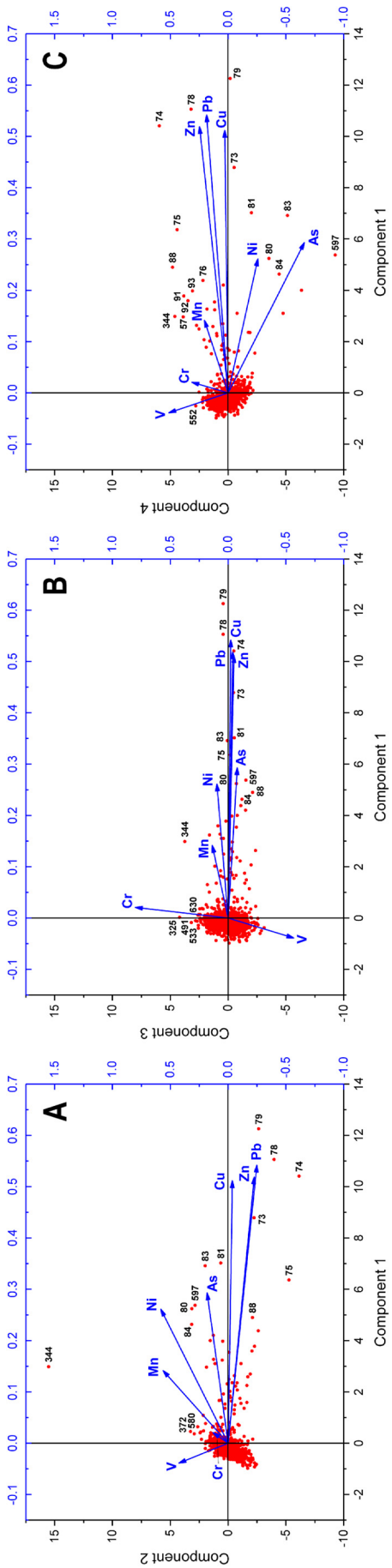

Fig. 4. Biplots of sampling points and component 1 with component 2 (A), component 3 (B) and component 4 (C) based on the principal component analysis.

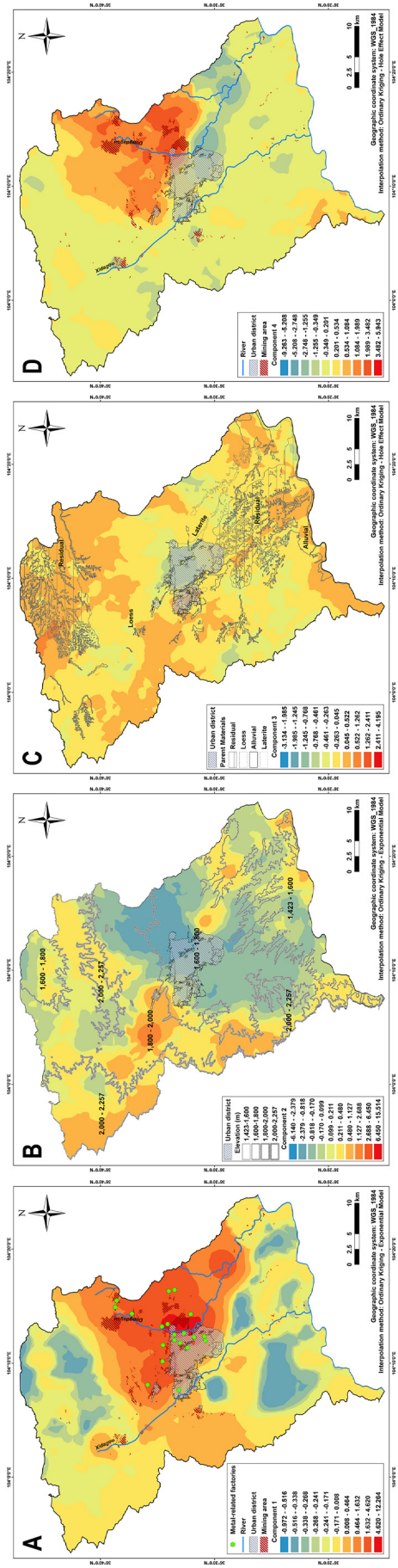

Fig. 5. Spatial distribution diagrams for component 1 (A), component 2 (B), component 3 (C) and component 4 (D) from principal component analysis drawn by using Ordinary Kriging interpolation in ArcGIS 10.

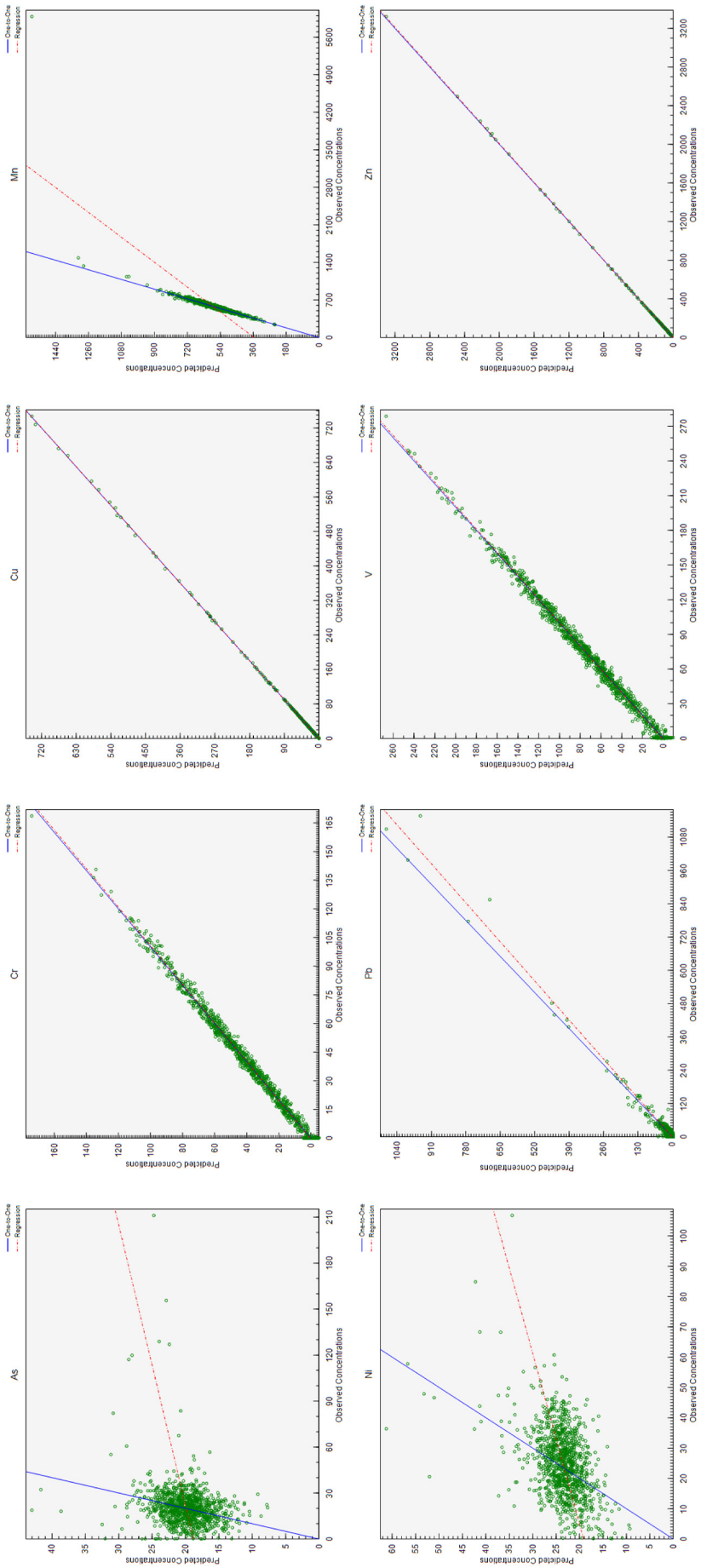

Fig. 6. Comparisons of observed concentrations and predicted values from the models in positive matrix factorization.

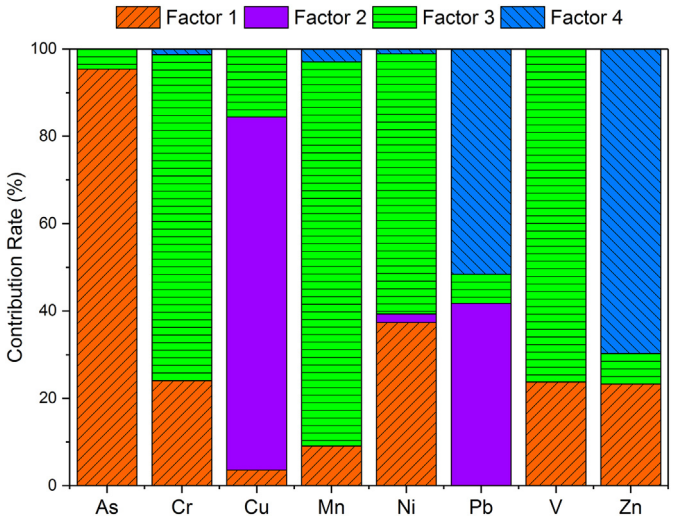

Fig. 7. Contribution rates of different sources on eight heavy metals based on positive matrix factorization.

and distribution of these heavy metals and to recognize their origins (Ha et al., 2014; Micó et al., 2006). The first six components explained 92.23% of the total variance with initial eigenvalues above 0.5 (Table S1). However, eight selected elements had high coefficients on the first four components. Lead (0.876), Zn (0.839), Cu (0.827), and As (0.573) related to the first principal component (32.68% of the total variance), indicating similar patterns in soil, whereas Ni (0.610) and Mn (0.589), Cr (0.821), and V (0.506) had high coefficients for the second (13.73%), third (13.15%), and fourth principal components (12.16%), respectively.

Three biplots are shown in Fig. 4, demonstrating the distinct properties of the eight heavy metals on the four components. For component 1, the common pattern of Pb, Zn, Cu, and As, was mainly expressed on points 79, 78, 74, 73 and 81, which were located in the outskirts and near the intensive industrial parks (Fig. 4A). This inferred that the four heavy metals were influenced substantially by human activities, especially mining and smelting in this region. The industrial waste outputs of water, gas, and solids were approximately 3.97×10^6 T, 9.61×10^{10} m^3, and 5.72×10^6 T; whereas the totals for residents were 3.60×10^7 T, 1.56×10^3 T, and 1.29×10^3 T per year, respectively (Statistics Bureau of Baiyin, 2017). These inputs might serve as the primary sources for soil contaminations (Alsaleh et al., 2018; Gabarrón et al., 2018).

Points 344, 372, 84, 80, and 580 had relatively high scores for component 2, scattering throughout the study area with no noticeable features discovered among them. These results indicated a lack of distinct characteristics on the distribution of Ni and Mn (Fig. 4A). Component 3, representing the dispersed trait of Cr, was revealed on points 325, 344, 491, 533, and 630, which also had an irregular rule (Fig. 4B). As for component 4, points 74, 88, 344, 75, and 57 displayed high eigenvalues and appeared in the vicinity of the city, indicating that this component was most likely controlled by anthropogenic origins (Fig. 4C) (Gabarrón et al., 2018).

3.5. Geographic information system

Spatial distribution diagrams for the four components were created based on the standardized scores of the sampling points, which were assigned to each component after PCA (Ha et al., 2014). The Yellow River in the south and mountains on the other three sides created an obvious natural border. Therefore, this boundary verified that no sample was collected outside the study area. After cross validation of all assigned sample locations, ordinary Kriging interpolation models selected in GIS were Exponential for component 1 and component 2, and Hole Effect for component 3 and component 4 (Fig. 5 and Table S2), according to the criterion of the minimum mean standardized (MS) of prediction errors and the closest to 1 of the root-mean-square error (RMSE) (Krivoruchko, 2011). Source identification was conducted by using these interpolation maps combined with the actual conditions of the sampling points (Facchinelli et al., 2001; Song et al., 2018).

Fig. 5A shows high-level plots for component 1 (colored with red) located in the outskirts and mining areas, where metal-related industrial parks were present. This area was famous for non-ferrous metals with 600 years of mining and smelting history (Baiyin District Portal, 2017; Nan et al., 1999); soils were polluted with Pb, Zn, Cu, and As from long-term and extensive non-ferrous metal production (Chakraborty et al., 2017). Component 1 (common patterns of Pb, Zn, Cu, and As), therefore, was not only influenced by the dominant natural background, but also controlled by industrial anthropogenic activities (mining and smelting).

In contrast with component 1, component 2 had low levels around the non-ferrous metal base and high levels in the northwest area of the map, indicating the different sources of Ni and Mn from the above four elements (Fig. 5B). These distribution phenomena roughly matched the altitude of the study region; areas with high scores appeared above 2000 m, whereas low values were located below 1600 m. This implied that movement of the earth's crust lifted the original rock rich in Ni and Mn via the orogenesis (Ding et al., 2017). Nickel and Mn were thus affected by natural factors such as rock weathering, which explained the distribution of component 2.

Relative homogeneity with subtle differences existed in the distribution of component 3 (Fig. 5C). Most of the study area had values close to zero, and the majority of the soils here were developed from Loess parent material. High score areas for component 3 were distributed at the north and the south of the map, where soils were formed from residual deposits (Brady and Weil, 1999). Component 3, representing Cr, therefore, was determined by soil parent materials (Huang et al., 2007; X. Zhang et al., 2018).

Component 4 consisted of high value regions concentrated in the mining areas (Fig. 5D). The high-level polygon did not expand into the urban district, nor did it extend down to the lower reaches of Dongdagou, a wastewater escape canal for metal-related factories and urban households (Chen et al., 2018; Wang et al., 2012). These results differed from component 1 suggesting that the element V was not controlled by anthropogenic activities, but originated from natural sources.

3.6. Positive matrix factorization

Positive Matrix Factorization was employed to quantify the contributions of different sources of heavy metals (Guan et al., 2018). The standard deviations of detected concentrations for each element at an individual point were chosen to be uncertainty data. Signal-to-Noise ratios (S/N) of As (1.5), Cr (2.6), Cu (2.5), Mn (9.6), Ni (1.6), Pb (1.4), V (2.0), and Zn (7.6) were all above 1, revealing the variabilities in the measurements were real. These revised ratios were calculated as the sum of concentration exceeding the uncertainty divided by the sum of uncertainty values. According to the number of component in PCA, the number of factors in the base model runs was set to 4, making the models well-fitted with residuals normally distributed between +3 and −3 and R^2 above 0.7 (Fig. 6). Three methods (base model, base model displacement, and base model bootstrap) were conducted, and the base model bootstrap result was selected because of the broadest error estimation, capturing both random errors and rotational ambiguity, in reference to the user guide of PMF 5.0 (U.S. EPA, 2014).

The results of average contribution rates for sources of heavy metals and factor profiles for sampling points are exhibited in Figs. 7 and S1. Based on the values of factor profiles, Ordinary Kriging in GIS was adopted to predict the distribution of these factors (Fig. 8). With the combination of these two approaches, the sources were identified and quantified. The majority of As came from factor 1, which displayed the

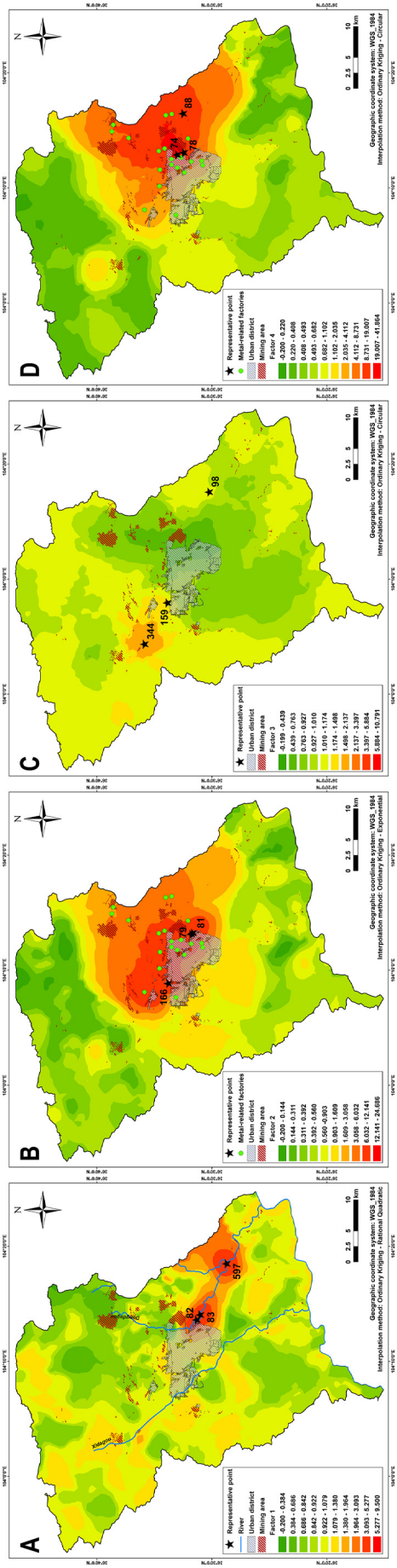

Fig. 8. Spatial distribution diagrams for factor 1 (A), factor 2 (B), factor 3 (C) and factor 4 (D) from positive matrix factorization drawn by using Ordinary Kriging interpolation in ArcGIS 10.

distribution of high-level blocks in the downstream basin of Dongdagou (Fig. 8A). For example, representative points 597, 82, and 83 with the highest value for factor 1, were located in a sewage irrigation area. Previous studies found Dongdagou was polluted by wastewater from mining areas and industrial zones, and the contaminated water was the primary irrigation resource for crop production along the river (Chen et al., 2018; Dai et al., 2012). It can be inferred that factor 1 was related to agricultural activities, and approximately 95.38% of As in soil originated from wastewater irrigation, which was accorded with the As distribution in this area (Fig. S2A).

Chromium, Mn, Ni, and V had a relatively consistent source, which was predominately controlled by factor 3, with percentages of 74.64, 88.01, 59.63, and 76.20%, respectively. As shown in Fig. 8C, three representative points (344, 159, and 98) for factor 3 are sporadically distributed in the area, illustrating that factor 3 denotes the natural origins including crustal movement, rock weathering, and soil parent material (Gu et al., 2012; Liu, 2017). Compared with the results of EF (Mn, V, and Ni derived from weathering processes and Cr derived from the Earth's crust), the outcomes of PCA and GIS (Ni and Mn derived from rock weathering, Cr came from parent materials, and V rooted from natural sources), along with the spatial distributions of the four elements (Fig. S2B, D, E, and G), the results were consistent and credible.

Factor 2 and factor 4 denoted two kinds of industrial sources from Cu/Pb and Pb/Zn factories, because the representative points 81, 166, 79 and 74, 78, 88 appeared within the intensive industrial parks in the outskirts (Fig. 8B and D). Currently, Cu, Pb, and Zn had a close link to the industrial discharge, such as mining and smelting factories, coal-fired power plants, and industrial zones (Shen et al., 2017; Yoon et al., 2006). The results followed the outcomes of the EF, PCA, GIS, and distributions of Cu, Pb, and Zn (Fig. S2C, F, and H), and also agreed with previous studies (Ha et al., 2014; Hu and Cheng, 2013; X. Zhang et al., 2018). Therefore, it could be concluded that the portions of 80.87, 93.34, and 69.71% of Cu, Pb, and Zn were derived from the industrial sources, respectively.

3.7. Comparison of multiple methods

The spatial deviation was a quick approach to obtain the general features of heavy metal distributions and to confirm the exogenous input of elements with high standard deviation and coefficient of variation (Jia et al., 2018; Tume et al., 2018). In the current study, the external input of Cu, Pb, and Zn in soils was found based on the spatial deviation. Correlation analysis was used to explore the common patterns of elements. Once the source of one item was confirmed, the elements with positive or negative relationships could be identified as similar or conflicting sources (Franco-Uría et al., 2009; Huang et al., 2007; Micó et al., 2006). Given this discipline, the consistent source of Cu, Mn, Pb, and Zn was determined. Calculated based on a reference element, EF was adopted to classify the sources of weathering processes or anthropogenic effects (Gu et al., 2012; Zhang and Liu, 2002). When the concentrations of a reference element dramatically changed, the judgment criterion for source needed to be correspondingly adjusted. According to the adjusted classification of EF values, it was determined that Zn, As, Cu, and Pb were from artificial sources, Mn, V, and Ni were from weathering processes, and Cr was from the natural background. While the three methods, SD, CA, and EF were all direct and convenient approaches for source identification, however, they could not pinpoint the exact sources and were not able to estimate the contributions of distinct sources.

To identify the sources by dimension reduction, PCA was conducted, obtaining different principal components with high variance explanation and corresponding standard scores (Das et al., 2018; Lü et al., 2018). Four components, representing four origins, were determined in this study. With the combination of spatial interpolation distribution of the component scores in GIS (Ha et al., 2014), the various sources were recognized, which Pb, Zn, Cu and As were from long-term metal production and Ni, Mn, Cr, and V were from natural sources such as rock weathering and parent materials. Although the sources have been determined, the contribution rates could not be directly achieved, because component scores derived from ordinary PCA had negative values that could not be calculated to the contribution rates, also the combination of regression analysis was to needed for contributor quantification (Huang et al., 2018; Xu et al., 2014). Differed from PCA, the positive factor profiles derived from PMF were directly utilized to calculate the contribution rates and to draw the spatial distribution diagrams in GIS for source identification (Guan et al., 2018; Tian et al., 2018). Furthermore, the introduction of uncertainty data improved the accuracy of identification of potential sources (U.S. EPA, 2014). The precise origins and exact contributions were confirmed by the combination of PMF and GIS, which were As (95%) from wastewater irrigation, Cr (75%), Mn (88%), Ni (60%), and V (76%) from natural origins, and Cu (81%), Pb (93%), and Zn (70%) from industrial sources. Therefore, combining these applications with the utilization of distribution maps and the real condition were accurate and essential for source apportionment of heavy metals in the soil.

4. Conclusions

Multiple methods, such as spatial deviation, correlation analysis, enrichment factor, principal component analysis, geographic information system, and positive matrix factorization, were employed to diagnose the sources of heavy metals in soils. After comparison, the combined applications of PMF, GIS, and PCA were accurate, applicable, and effective for source determination.

Three origins were identified and exact contributions were calculated: 95.38% of As came from wastewater irrigation; 74.64, 88.01, 59.63, and 76.20% of Cr, Mn, Ni, and V, respectively, were derived from natural origins, such as crustal movement, rock weathering, and soil parent material; 80.87, 93.34, and 60.71% of Cu, Pb, and Zn, respectively, came from the industrial sources. Natural origins, industrial sources, and wastewater irrigation were the three main contributions to heavy metals in cropland soils from this region.

For this resource-based region, where soils were heavily contaminated with As, Cu, Pb, and Zn, anthropogenic activities including industrial input and wastewater irrigation were the predominant source of pollution in cropland. The key to tackling this severe issue is to reduce the contaminant discharge in industrial areas and to improve the quality of irrigation water. Therefore, the results are of great significance in guiding prevention-controlling-remediation strategies for heavy metal contamination in the local land.

Acknowledgements

This study was funded by the National Science & Technology Support Program (2012BAD05B03), the National Key Technology Research & Development Program of China (2016YFD0200101, 2017YFD0800900), the Gansu Natural Science Foundation (1606RJZA111), the Science & Technology Innovation Plan of Gansu Academy of Agricultural Sciences (2017GAAS28), and the Shandong Provincial Key Research and Development Program (2016CYJS05A02).

Appendix A. Supplementary data

Supplementary data to this article can be found online at https://doi.org/10.1016/j.scitotenv.2018.10.130.

References

Alsaleh, K.A.M., Meuser, H., Usman, A.R.A., Al-Wabel, M.I., Al-Farraj, A.S., 2018. A comparison of two digestion methods for assessing heavy metals level in urban soils influenced by mining and industrial activities. J. Environ. Manag. 206, 731–739. https://doi.org/10.1016/j.jenvman.2017.11.026.

Baiyin District Portal, 2017. Introduction of Baiyin District. http://www.baiyinqu.gov.cn/cms/item-list-category-743.shtml, Accessed date: 4 June 2018.
Brady, N.C., Weil, R.R., 1999. The Nature and Properties of Soils. Prentice-Hall Inc., Upper Saddle River, New Jersey, pp. 38–51.
Cai, L., Stephen, Y., Sun, C., Cai, X., Zhang, R., 2015. GIS-based assessment of arable layer pollution of copper (Cu), zinc (Zn) and lead (Pb) in Baiyin District of Gansu Province. Environ. Earth Sci. 74, 803–811. https://doi.org/10.1007/s12665-015-4084-5.
Carr, R., Zhang, C., Moles, N., Harder, M., 2008. Identification and mapping of heavy metal pollution in soils of a sports ground in Galway City, Ireland, using a portable XRF analyser and GIS. Environ. Geochem. Health 30, 45–52. https://doi.org/10.1007/s10653-007-9106-0.
Chakraborty, S., Man, T., Paulette, L., Deb, S., Li, B., Weindorf, D.C., Frazier, M., 2017. Rapid assessment of smelter/mining soil contamination via portable X-ray fluorescence spectrometry and indicator kriging. Geoderma 306, 108–119. https://doi.org/10.1016/j.geoderma.2017.07.003.
Chen, Y., Jiang, Y., Huang, H., Mou, L., Ru, J., Zhao, J., Xiao, S., 2018. Long-term and high-concentration heavy-metal contamination strongly influences the microbiome and functional genes in Yellow River sediments. Sci. Total Environ. 637–638, 1400–1412. https://doi.org/10.1016/j.scitotenv.2018.05.109.
CNEMC, 1990. Background Values of Soil Elements in China. China National Environmental Monitoring Centre. China Environmental Science Press, Beijing (in Chinese).
CNMEP, 2015. Soil and Sediment - Determination of Inorganic Element - Wavelength Dispersive X-Ray Fluorescence Spectrometry. HJ 780–2015. M.O.E.P, China.
CNMF & CNMEP, 2015. Key Areas for the Prevention and Control of Heavy Metal Contamination in 2015. Chinese Ministry of Finance and Chinese Ministry of Environmental Protection http://jjs.mof.gov.cn/zhengwuxinxi/tongzhigonggao/201506/t20150602_1248397.html, Accessed date: 4 June 2018.
Dai, X.P., Feng, L., Ma, X.W., Zhang, Y.M., 2012. Concentration level of heavy metals in wheat grains and the health risk assessment to local inhabitants from Baiyin, Gansu, China. Adv. Mater. Res. 518-523, 951–956. https://doi.org/10.4028/www.scientific.net/AMR.518-523.951.
Das, A., Patel, S.S., Kumar, R., Krishna, K.V.S.S., Dutta, S., Saha, M.C., Sengupta, S., Guha, D., 2018. Geochemical sources of metal contamination in a coal mining area in Chhattisgarh, India using lead isotopic ratios. Chemosphere 197, 152–164. https://doi.org/10.1016/j.chemosphere.2018.01.016.
Ding, Q., Cheng, G., Wang, Y., Zhuang, D., 2017. Effects of natural factors on the spatial distribution of heavy metals in soils surrounding mining regions. Sci. Total Environ. 578, 577–585. https://doi.org/10.1016/j.scitotenv.2016.11.001.
Du, C., Liu, E., Chen, N., Wang, W., Gui, Z., He, X., 2017. Factorial kriging analysis and pollution evaluation of potentially toxic elements in soils in a phosphorus-rich area, south Central China. J. Geochem. Explor. 175, 138–147. https://doi.org/10.1016/j.gexplo.2017.01.010.
Edwards, A.C., 2010. Soil sampling and sample preparation. In: Hooda, P.S. (Ed.), Trace Elements in Soils. John Wiley & Sons Ltd, Chichester, pp. 39–51.
Facchinelli, A., Sacchi, E., Mallen, L., 2001. Multivariate statistical and GIS-based approach to identify heavy metal sources in soils. Environ. Pollut. 114, 313–324. https://doi.org/10.1016/S0269-7491(00)00243-8.
Franco-Uría, A., López-Mateo, C., Roca, E., Fernández-Marcos, M.L., 2009. Source identification of heavy metals in pastureland by multivariate analysis in NW Spain. J. Hazard. Mater. 165, 1008–1015. https://doi.org/10.1016/j.jhazmat.2008.10.118.
Gabarrón, M., Faz, A., Acosta, J.A., 2018. Use of multivariable and redundancy analysis to assess the behavior of metals and arsenic in urban soil and road dust affected by metallic mining as a base for risk assessment. J. Environ. Manag. 206, 192–201. https://doi.org/10.1016/j.jenvman.2017.10.034.
Gan, Y., Wang, L., Yang, G., Dai, J., Wang, R., Wang, W., 2017. Multiple factors impact the contents of heavy metals in vegetables in high natural background area of China. Chemosphere 184, 1388–1395. https://doi.org/10.1016/j.chemosphere.2017.06.072.
Gu, Y., Wang, Z., Lu, S., Jiang, S., Mu, D., Shu, Y., 2012. Multivariate statistical and GIS-based approach to identify source of anthropogenic impacts on metallic elements in sediments from the mid Guangdong coasts, China. Environ. Pollut. 163, 248–255. https://doi.org/10.1016/j.envpol.2011.12.041.
Gu, Y.G., Li, Q.S., Fang, J.H., He, B.Y., Fu, H.B., Tong, Z.J., 2014. Identification of heavy metal sources in the reclaimed farmland soils of the Pearl River estuary in China using a multivariate geostatistical approach. Ecotoxicol. Environ. Saf. 105, 7–12. https://doi.org/10.1016/j.ecoenv.2014.04.003.
Guan, Q., Wang, F., Xu, C., Pan, N., Lin, J., Zhao, R., Yang, Y., Luo, H., 2018. Source apportionment of heavy metals in agricultural soil based on PMF: a case study in Hexi corridor, Northwest China. Chemosphere 193, 189–197. https://doi.org/10.1016/j.chemosphere.2017.10.151.
Ha, H., Olson, J.R., Bian, L., Rogerson, P.A., 2014. Analysis of heavy metal sources in soil using kriging interpolation on principal components. Environ. Sci. Technol. 48, 4999–5007. https://doi.org/10.1021/es405083f.
Han, W., Gao, G., Geng, J., Li, Y., Wang, Y., 2018. Ecological and health risks assessment and spatial distribution of residual heavy metals in the soil of an e-waste circular economy park in Tianjin, China. Chemosphere 197, 325–335. https://doi.org/10.1016/j.chemosphere.2018.01.043.
Hu, Y., Cheng, H., 2013. Application of stochastic models in identification and apportionment of heavy metal pollution sources in the surface soils of a large-scale region. Environ. Sci. Technol. 47, 3752–3760. https://doi.org/10.1021/es304310k.
Hu, Y., Nan, Z., 2018. Soil contamination in arid region of Northwest China: status mechanism and mitigation. In: Luo, Y., Tu, C. (Eds.), Twenty Years of Research and Development on Soil Pollution and Remediation in China. Springer Singapore, Singapore, pp. 365–374.
Hu, B., Wang, J., Jin, B., Li, Y., Shi, Z., 2017. Assessment of the potential health risks of heavy metals in soils in a coastal industrial region of the Yangtze River Delta. Environ. Sci. Pollut. Res. 24, 19816–19826. https://doi.org/10.1007/s11356-017-9516-1.
Huang, S.S., Liao, Q.L., Hua, M., Wu, X.M., Bi, K.S., Yan, C.Y., Chen, B., Zhang, X.Y., 2007. Survey of heavy metal pollution and assessment of agricultural soil in Yangzhong district, Jiangsu Province, China. Chemosphere 67, 2148–2155. https://doi.org/10.1016/j.chemosphere.2006.12.043.
Huang, Y., Deng, M., Wu, S., Japenga, J., Li, T., Yang, X., He, Z., 2018. A modified receptor model for source apportionment of heavy metal pollution in soil. J. Hazard. Mater. 354, 161–169. https://doi.org/10.1016/j.jhazmat.2018.05.006.
Jia, Y., Wang, L., Qu, Z., Yang, Z., 2018. Distribution, contamination and accumulation of heavy metals in water, sediments, and freshwater shellfish from Liuyang River, Southern China. Environ. Sci. Pollut. Res. 25, 7012–7020. https://doi.org/10.1007/s11356-017-1068-x.
Kabata-Pendias, A., 2011. Trace Elements in Soils and Plants. CRC Press, Taylor & Francis Group, Boca Raton.
Krivoruchko, K., 2011. Spatial Statistical Data Analysis for GIS Users. Esri Press Redlands.
Li, Y., Wang, Y.B., Gou, X., Su, Y.B., Wang, G., 2006. Risk assessment of heavy metals in soils and vegetables around non-ferrous metals mining and smelting sites, Baiyin, China. J. Environ. Sci. (China) 18, 1124–1134. https://doi.org/10.1016/S1001-0742(06)60050-8.
Liu, Z.P., 2003. Lead poisoning combined with cadmium in sheep and horses in the vicinity of non-ferrous metal smelters. Sci. Total Environ. 309, 117–126. https://doi.org/10.1016/S0048-9697(03)00011-1.
Liu, B., 2017. Heavy Metal Contamination in Farmland Soils and its Transfer in the Soil-Crop-Human System Within the Dongdagou Watershed, Baiyin, Gansu. (Dissertation). Lanzhou University (in Chinese, with an English abstract).
Lü, J., Jiao, W., Qiu, H., Chen, B., Huang, X., Kang, B., 2018. Origin and spatial distribution of heavy metals and carcinogenic risk assessment in mining areas at You'xi county Southeast China. Geoderma 310, 99–106. https://doi.org/10.1016/j.geoderma.2017.09.016.
Luque-Espinar, J.A., Pardo-Igúzquiza, E., Grima-Olmedo, J., Grima-Olmedo, C., 2018. Multiscale analysis of the spatial variability of heavy metals and organic matter in soils and groundwater across Spain. J. Hydrol. 561, 348–371. https://doi.org/10.1016/j.jhydrol.2018.04.013.
McGladdery, C., Weindorf, D.C., Chakraborty, S., Li, B., Paulette, L., Podar, D., Pearson, D., Kusi, N.Y.O., Duda, B., 2018. Elemental assessment of vegetation via portable X-ray fluorescence (PXRF) spectrometry. J. Environ. Manag. 210, 210–225. https://doi.org/10.1016/j.jenvman.2018.01.003.
Micó, C., Recatalá, L., Peris, M., Sánchez, J., 2006. Assessing heavy metal sources in agricultural soils of an European Mediterranean area by multivariate analysis. Chemosphere 65, 863–872. https://doi.org/10.1016/j.chemosphere.2006.03.016.
Nan, Z., Zhao, C., 2000. Heavy metal concentrations in gray calcareous soils of Baiyin region, Gansu Province, P.R. China. Water Air Soil Pollut. 118, 131–142. https://doi.org/10.1023/A:1005135618750.
Nan, Z.R., Zhao, C.Y., Li, J.J., Chen, F.H., Liu, Y., 1999. Field survey of Cd and Pb contents in spring wheat (*Triticum aestivum* L.) grain grown in Baiyin City, Gansu province, People's Republic of China. Bull. Environ. Contam. Toxicol. 63, 546–552. https://doi.org/10.1007/s001289901015.
Nan, Z., Zhao, C., Li, J., Chen, F., Sun, W., 2002. Relations between soil properties and selected heavy metal concentrations in spring wheat (*Triticum aestivum* L.) grown in contaminated soils. Water Air Soil Pollut. 133, 205–213. https://doi.org/10.1023/A:1012962604095.
Pearson, D., Weindorf, D.C., Chakraborty, S., Li, B., Koch, J., Van Deventer, P., de Wet, J., Kusi, N.Y., 2018. Analysis of metal-laden water via portable X-ray fluorescence spectrometry. J. Hydrol. 561, 267–276. https://doi.org/10.1016/j.jhydrol.2018.04.014.
Ranjan, P., Ramanathan, A.L., Kumar, A., Singhal, R.K., Datta, D., Venkatesh, M., 2018. Trace metal distribution, assessment and enrichment in the surface sediments of Sundarban mangrove ecosystem in India and Bangladesh. Mar. Pollut. Bull. 127, 541–547. https://doi.org/10.1016/j.marpolbul.2017.11.047.
Shen, F., Liao, R., Ali, A., Mahar, A., Guo, D., Li, R., Xining, S., Awasthi, M.K., Wang, Q., Zhang, Z., 2017. Spatial distribution and risk assessment of heavy metals in soil near a Pb/Zn smelter in Feng County, China. Ecotoxicol. Environ. Saf. 139, 254–262. https://doi.org/10.1016/j.ecoenv.2017.01.044.
Song, H., Hu, K., An, Y., Chen, C., Li, G., 2018. Spatial distribution and source apportionment of the heavy metals in the agricultural soil in a regional scale. J. Soils Sediments 18, 852–862. https://doi.org/10.1007/s11368-017-1795-0.
Statistics Bureau of Baiyin, 2017. Baiyin Statistics Yearbook of 2016. Statistics Bureau of Baiyin, Baiyin (in Chinese).
Tang, Z., Bai, Y., Li, Z., 2002. Geotectonic settings of large and Superlarge mineral deposits on the southwestern margin of the North China plate. Acta Geol. Sin. 76, 367–377. https://doi.org/10.1111/j.1755-6724.2002.tb00553.x.
Tian, S., Liang, T., Li, K., Wang, L., 2018. Source and path identification of metals pollution in a mining area by PMF and rare earth element patterns in road dust. Sci. Total Environ. 633, 958–966. https://doi.org/10.1016/j.scitotenv.2018.03.227.
Tighe, M., Rogan, G., Wilson, S.C., Grave, P., Kealhofer, L., Yukongdi, P., 2018. The potential for portable X-ray fluorescence determination of soil copper at ancient metallurgy sites, and considerations beyond measurements of total concentrations. J. Environ. Manag. 206, 373–382. https://doi.org/10.1016/j.jenvman.2017.10.052.
Tume, P., Roca, N., Rubio, R., King, R., Bech, J., 2018. An assessment of the potentially hazardous element contamination in urban soils of Arica, Chile. J. Geochem. Explor. 184, 345–357. https://doi.org/10.1016/j.gexplo.2016.09.011.
U.S. EPA, 2014. EPA Positive Matrix Factorization (PMF) 5.0 Fundamentals and User Guide. EPA/600/R-14/108. U.S. Environmental Protection Agency.
Wang, S., Nan, Z., Xue, S., Li, P., Wang, D., Liao, Q., Cao, Z., 2012. Speciation and Risk Assessment of Cd, Zn, Pb, Cu and Ni in Surface Sediments of Dongdagou Stream, Baiyin, China. IEEE, pp. 1–4.
Wikipedia. Baiyien. https://en.wikipedia.org/wiki/Baiyin, Accessed date: 24 May 2018.
Xu, X., Zhao, Y., Zhao, X., Wang, Y., Deng, W., 2014. Sources of heavy metal pollution in agricultural soils of a rapidly industrializing area in the Yangtze Delta of China. Ecotoxicol. Environ. Saf. 108, 161–167. https://doi.org/10.1016/j.ecoenv.2014.07.001.

Yang, D., Gao, X., Xu, L., Guo, Q., 2018. Constraint-adaptation challenges and resilience transitions of the industry–environmental system in a resource-dependent city. Resour. Conserv. Recycl. 134, 196–205. https://doi.org/10.1016/j.resconrec.2018.03.016.

Yoon, J., Cao, X., Zhou, Q., Ma, L.Q., 2006. Accumulation of Pb, Cu, and Zn in native plants growing on a contaminated Florida site. Sci. Total Environ. 368, 456–464. https://doi.org/10.1016/j.scitotenv.2006.01.016.

Zhang, J., Liu, C.L., 2002. Riverine composition and estuarine geochemistry of particulate metals in China—weathering features, anthropogenic impact and chemical fluxes. Estuar. Coast. Shelf Sci. 54, 1051–1070. https://doi.org/10.1006/ecss.2001.0879.

Zhang, Q., Wang, S., Nan, Z., Li, Y., Zang, F., 2018. Accumulation, fractionation, and risk assessment of mercury and arsenic in the soil-wheat system from the wastewater-irrigated soil in Baiyin, Northwest China. Environ. Sci. Pollut. Res. 25, 14856–14867. https://doi.org/10.1007/s11356-018-1641-y.

Zhang, X., Wei, S., Sun, Q., Wadood, S.A., Guo, B., 2018. Source identification and spatial distribution of arsenic and heavy metals in agricultural soil around Hunan industrial estate by positive matrix factorization model, principle components analysis and geo statistical analysis. Ecotoxicol. Environ. Saf. 159, 354–362. https://doi.org/10.1016/j.ecoenv.2018.04.072.

Zoller, W.H., Gladney, E.S., Duce, R.A., 1974. Atmospheric concentrations and sources of trace metals at the south pole. Science 183, 198–200. https://doi.org/10.1126/science.183.4121.198.